Porosity and crystallization of water ice films studied by positron and positronium annihilation

Y. C. Wu,[1,2] J. Jiang,[1] S. J. Wang,[1] A. Kallis,[2] and P. G. Coleman[2,*]

[1]*School of Physics and Technology, Hubei Nuclear Solid Physics Key Laboratory, Wuhan University, Wuhan 430072, People's Republic of China*

[2]*Department of Physics, University of Bath, Bath BA2 7AY, United Kingdom*

(Received 25 May 2011; revised manuscript received 14 July 2011; published 29 August 2011)

The growth, evolution, and annealing of closed and interconnected pores in amorphous and crystalline films of water ice grown under a range of conditions have been studied by variable-energy positron annihilation spectroscopy (VEPAS). By measuring positron and positronium-related annihilation parameters as a function of time and film temperature it is shown that VEPAS has the capacity to yield a wealth of depth-dependent information on film morphology, with particularly promising results on the evolution and annealing of subnanometer closed pores—inaccessible to other techniques—and the study of the energetics of structural and phase changes.

DOI: 10.1103/PhysRevB.84.064123 PACS number(s): 61.43.Gt, 64.70.D−, 68.55.J−, 78.70.Bj

I. INTRODUCTION

Ice, the condensed phase of water, exists not only on the surface of Earth but also throughout our planetary system and interstellar space.[1] The reactivity of the ice surface is sensitive to its structure; amorphous solid water (ASW) is the most abundant phase of water in astrophysical environments and, as a metastable extension of liquid water, is a model system for studying deeply supercooled liquids.[2] It is well known that the physical properties of ASW are strongly influenced by growth and annealing procedures (e.g., Ref. 3). Water vapor deposited on a substrate held at a temperature below 130 K forms low-density ASW, which is thermodynamically unstable, and which above 135 K transforms to a stable crystalline cubic ice (CI).[4] Unanswered questions remain; for example, phase transition temperatures[5] and the initiation of crystallization.[6,7]

Both ASW and CI films can be deposited in the laboratory by introducing water vapor through a needle valve into an evacuated vessel in which is mounted a cold substrate. The physical properties of slow-grown films—e.g., porosity, average density, crystallinity—have been shown to depend on the temperature of the substrate during growth. Below ∼110 K highly porous, low-density films are grown, which irreversibly densify on annealing; between 110 and 120 K compact (low- or zero-porosity) films result, with average densities of ∼0.85 g cm^{-3}, and crystalline films are grown at 140–160 K.[8]

Research into the many unusual properties of ASW is being widely pursued, including the growth, nature, and destruction of pores.[3,9,10–12] The adsorption and desorption of molecular gases by micropores (of diameter below ∼2 nm) in ASW films has been studied using a variety of techniques.[8,10,13–17] However, when pores are too small, or not connected to the sample surface, such gas measurements are ineffective.

Positrons and positronium (Ps), the bound state of a positron with an electron, are highly sensitive to open volume in a material, ranging from monovacancies (via positron trapping) to pores of several nanometers in diameter (via Ps formation and decay). In variable-energy positron annihilation spectroscopy (VEPAS)[18] positrons are implanted in a sample to a chosen mean depth (∼40 $E^{1.6}$ nm, with E in keV, for a material of unit density) and by measuring the characteristics of positron and/or Ps annihilation radiation one can study defects and pores in thin films.[19,20] When positrons are trapped in open volume clusters of up to ∼20 missing atoms, their annihilation radiation is measurably different from that of an untrapped positron; however, in larger pores (∼nm size) the positron wave function is no longer effectively constricted and the positron behaves as a free particle encountering a cleaner inner surface. In a larger cavity, however, Ps may form and, if in the longer-lived *ortho* (spin triplet) state (*o*-Ps), the fraction of *o*-Ps which survives to decay naturally into three γ rays depends on the size of the void, and/or the extent to which voids are interconnected and provide pathways to the vacuum above the surface.[21] The spin-singlet form *para* Ps (*p*-Ps) decays, like positrons, with the emission of two γ rays.

The only previous reports of the application of VEPAS to ice films are those of Eldrup *et al.*,[22,23] who measured the Ps diffusion coefficients in crystalline and amorphous ice (0.2 and 10^{-3} cm^2 s^{-1}, respectively), and the present authors, who observed near-surface and bulk crystallization, and pore collapse in ice films grown at 50 K.[24]

In the present work the initial studies of Wu *et al.*[24] are extended to include the study by VEPAS of both crystalline and amorphous ice, measuring both the yield of 3γ (*o*-Ps) annihilation radiation and the Doppler broadening of (positron) annihilation line shape for films grown and annealed over the temperature range 50–170 K. Structural changes on or near the surface of ice are important since transport properties and adsorption (desorption) behavior are strongly related to such phenomena; therefore, the structure, porosity, and crystallization of water ice films grown at different deposition temperatures have been investigated. While the current measurements can provide qualitative information on the formation and evolution of micropores ($<\sim$2 nm diam) and mesopores (∼2–50 nm diam), quantitative assignment of pore sizes and concentrations awaits the resolution of a number of experimental issues,[25] and this will be a focus of future work.

II. EXPERIMENT

Porous ASW films were grown on a semicylindrical copper block, cooled by a closed-cycle He cryostat to 50 K, compact (nonporous) films at 120 K, and CI films at 150 K. The

thickness of the films was 8-10 μm unless stated, and the growth time was ∼15 h. The base pressure in the positron beam system[26] was $\sim 10^{-6}$ Pa. Deionized water in a side chamber was first degassed via a number of freeze-pump-thaw cycles and water vapor introduced at a controllable rate into the sample chamber through a needle valve. The sample temperature was controlled to within ±1 K in the range 50–170 K by the cryostat system. Both ASW and CI samples were grown at fast (∼500 nm min^{-1}) and slow (approximately a few nm min^{-1}) rates and their thicknesses were thereby controllable.

Annihilation γ energy spectra were recorded for incident positron energies E from 0.25 to 30 keV (corresponding to mean implantation depths from the surface to ∼10 μm) by a high-purity Ge detector system. The conventional S and W parameters, and the $3\gamma : 2\gamma$ ratio parameter R were deduced from the spectra; these parameters are sensitive to positron annihilation with low- and high-momentum electrons, and to the fraction of positrons decaying as o-Ps into three γ rays, respectively. S and W were deduced from the central and wing fractions of the 511-keV annihilation γ peak, containing typically 10^6 events, and R from the ratio of the annihilation events recorded in the "valley" region between 475 and 505 keV to those in the 511-keV peak. The parameter F, proportional to the fraction of implanted positrons annihilated as Ps, was then found from $F = (R - R_0)/(R_1 - R_0)$, where R_0 is the value of R when no Ps is formed (e.g., in copper at $E = 30$ keV), and R_1 is the maximum value of R measured in the current experiment (at the lowest E). Annihilation parameters and positron (Ps) diffusion lengths were obtained by fitting raw data (i.e., S and F versus E) with the code VEPFIT.[27]

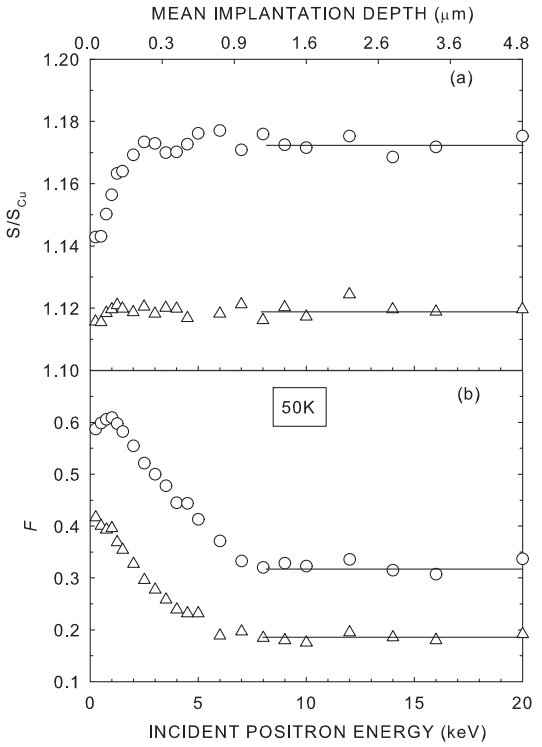

FIG. 1. (a) S/S_{Cu} and (b) F versus incident positron energy E for ASW films fast and slow grown at 50 K (circles and triangles, respectively). The mean positron implantation depth in a solid of unit density is shown on the upper horizontal axis for guidance only. S values are normalized to the value for the Cu substrate.

III. RESULTS AND DISCUSSION

A. Growth of ASW and CI films

$S(E)/S_{\text{Cu}}$ and $F(E)$ for ASW films grown at 50 K at rates of approximately a few nm min^{-1} and ∼ 500 nm min^{-1} are shown in Fig. 1. The S values are normalized to the value for the bulk copper substrate. The mean implantation depth of positrons in a film of unit density is shown on the upper horizontal axis.

These films are expected to be highly porous. At all E the measured F and S values are considerably higher for the fast-grown film, indicating the existence of more open and closed pores in this film. The changes in F and S at low energies reflect the diffusion of o-Ps and positrons (p-Ps) to the surface, respectively (through ice or via open channels). F reaches its asymptotic value over a wider range of E than S because the effective diffusion length of o-Ps is higher than that of positrons or p-Ps, both of which have a much shorter mean lifetime (∼10^2 ps versus ∼10^2 ns). The roughly flat $F(E)$ below 1 keV for the fast-grown film suggests that all o-Ps formed at shallow depths are able to escape to the vacuum. As described in Ref. 24, one can obtain a relative measure of the diffusion of o-Ps to the surface by fitting $F(E)$ using the code VEPFIT, giving effective Ps diffusion (migration) lengths L_{Ps} of ∼200 and 150 nm for the fast- and slow-grown films, respectively. These values, coupled with the relatively high surface and bulk values of F for both films, are consistent with the films being of high porosity with a network of interconnected pores.

Figure 2 shows $S(E)/S_{\text{Cu}}$ and $F(E)$ films grown at 120 K at approximately the same two rates as the 50 K films in Fig. 1. The markedly lower F values indicate that these films are much less porous than those grown at 50 K, in agreement with Ref. 8; the fitted L_{Ps} are only ∼15 and 35 nm for the fast- and slow-grown films, respectively. However, the nonzero values of F and the still-high values of S suggest that these films do contain a relatively high concentration of smaller, closed pores. The higher F value in slow-grown film implies that more, or some larger (interconnected), pores exist in what would normally be termed a "compact" film.

The results for CI films grown at 150 K at the same rates are shown in Fig. 3. The thickness of the slow-grown film is only ∼400 nm and so S decreases above ∼7 keV towards unity, the substrate value. The high S in the films comes from p-Ps annihilation, 2γ "quenched" o-Ps annihilation, and the annihilation of positrons trapped in any crystal defects. Compared to the compact films grown at 120 K, the high F near the surface (i.e., at low E) is due to the longer L_{Ps} in CI[21]: fitted L_{Ps} values are ∼40 and 60 nm for fast- and slow-grown films. The very low but nonzero value of F for the bulk CI film implies that either o-Ps is forming and decaying into three γ rays within larger closed pores in the crystal, or perhaps a few percent of o-Ps atoms are diffusing to the surface even from the bulk. The higher F for the fast-grown film implies the existence of mesopores or open pores in this film.

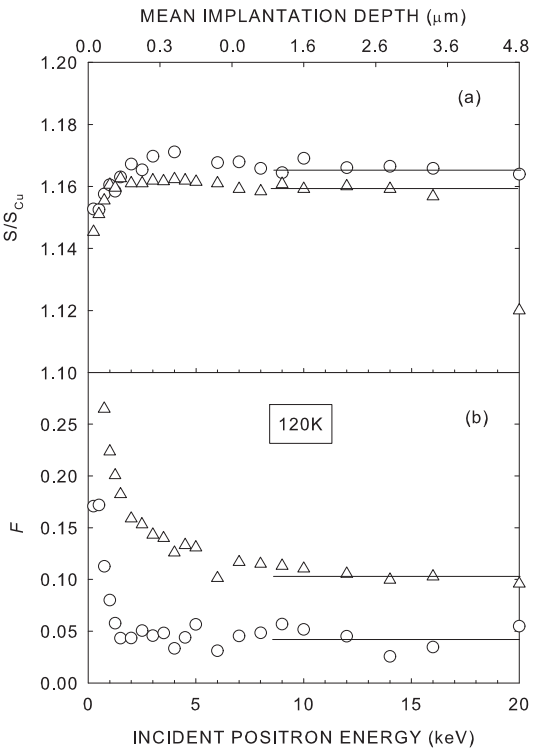

FIG. 2. (a) $S(E)/S_{\mathrm{Cu}}$ and (b) $F(E)$ for ASW films fast and slow grown at 120 K (circles and triangles, respectively).

B. Time and temperature effects

Figure 4 shows S/S_{Cu} and F as function of time for the near-surface layer ($E = 1$ keV, equivalent to a mean implanted depth of 40 nm) and in the bulk film ($E = 4$ and 30 keV, equivalent to mean implanted depths of 0.4 and 10 μm). Repeated 500-s measurements were made at 50 and 150 K, starting immediately after the growth of ASW and CI films at those temperatures. For both films it is interesting to note that the near-surface F decreases with time, reaching an asymptotic value after almost 30 h. The near-surface S shows a similar behavior, but exhibits a smaller change. In contrast, F and S in the bulk films do not change with time.

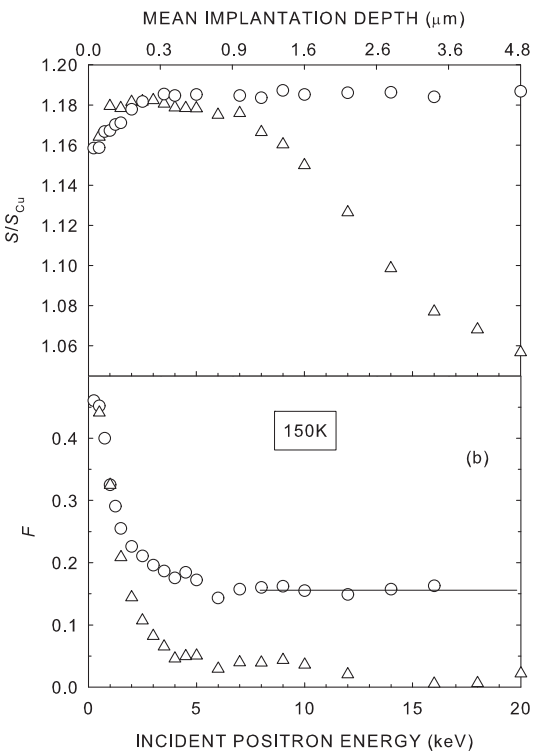

FIG. 3. (a) $S(E)/S_{\mathrm{Cu}}$ and (b) $F(E)$ for ASW films fast and slow grown at 150 K (circles and triangles, respectively).

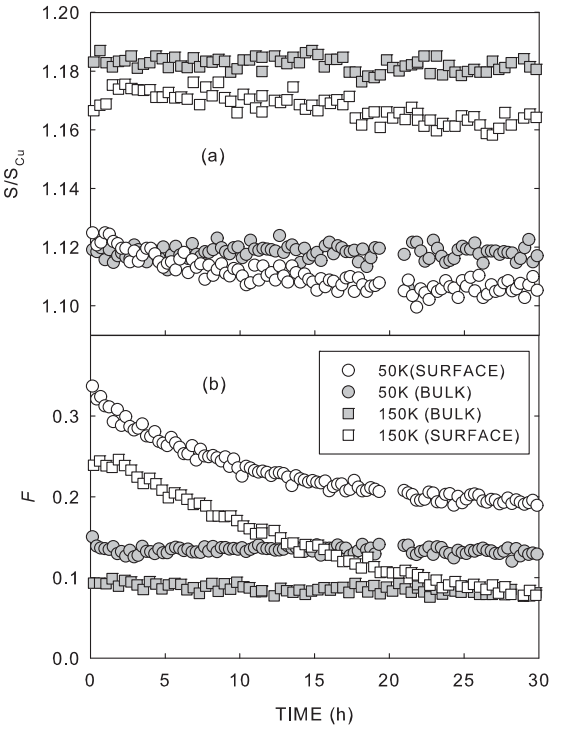

FIG. 4. (a) $S(t)/S_{\mathrm{Cu}}$ and (b) $F(t)$ for as-grown ASW and CI films grown at 50 and 150 K, respectively.

These measurements suggest that the surfaces of the as-grown films are both very irregular and unstable, and that the topmost layers of ice undergo a microstructural transformation due to the reorganization of water molecules which may lead to the collapse of micropores. Such a collapse would greatly decrease the fraction of o-Ps able to reach the vacuum above the surface, hence decreasing the parameter F. The greater relative decrease in F and S seen at 150 K may reflect the higher molecular mobility at the higher temperature. Using ultra-low-energy Ar ion scattering Cyriac and Pradeep[5] found that the topmost layers of amorphous ice undergo a structural transformation before the onset of crystallization and well below 120 K; the present results suggest that reorganization of water molecules apparently takes place at temperatures as low as 50 K.

Figure 5 shows $F(E)$ for a CI film grown at 150 K and a CI film prepared by growth at 50 K and subsequent annealing at 150 K. The measurements were made at 50, 130, and 150 K. The results for the two films show similar features: (i) the zero-energy limit $F(0)$—reflecting the probability of three-γ Ps decay at or above the sample surface—increases with the measurement temperature, (ii) Ps towards the surface is characterized by largely temperature-independent fitted L_{Ps}

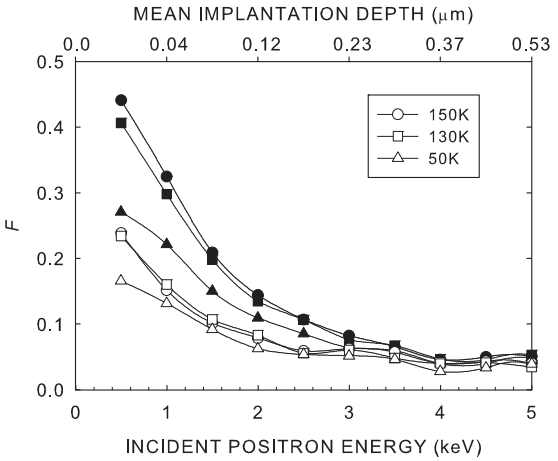

FIG. 5. Equilibrium $F(E)$ measured at 50, 130, and 150 K for CI films grown at 150 K (filled symbols) and grown at 50 K and annealed at 150 K (open symbols).

values of ∼45 and 65 nm for the films grown at 150 and 50 K, respectively, and (iii) the formation of Ps is reversible for a given film. $F(0)$ is higher in the film grown at 150 K, suggesting a difference between the near-surface pore structure of the two films.

Eldrup *et al.*[22,28] postulated that the temperature effects seen here in Fig. 5 might be primarily due to the temperature dependence of the slowing-down range of the excess electron. However, Sack and Baragiola,[29] using a piezoelectric microbalance and a mass spectrometer, found that ice films grown below 140 K had an enhanced sublimation rate which decayed in time and which depended on film thickness and growth temperatures. This model is consistent with the results of Figs. 4 and 5, and we consequently suggest that there is a direct correlation between $F(0)$ and the sublimation rate. For freshly grown films, the higher sublimation rate may accelerate reorganization of water molecules at the surface, inducing a morphological change in the near-surface region and, as the sublimation rate decreases, so does $F(0)$, as seen in Fig. 4. At lower temperatures the sublimation rate is lower (sublimation energy = 0.45 eV[29]) resulting in a lower $F(0)$ (Fig. 5).

C. Annealing of open and closed pores

$F(E)$ at different temperatures for an exemplar ASW film—several micrometers thick—grown at 50 K have been measured; similar results were obtained for a number of ASW films grown under different conditions. L_{Ps}, $F(0)$, and the bulk F_B obtained by fitting these data (for $E1$ keV) using VEPFIT are shown in Fig. 6 as a function of annealing temperature T. F_B is the high-E asymptotic value of $F(E)$. L_{Ps} falls from ∼160 nm at low temperatures to a minimum of ∼25 nm at 120 K, reflecting a decrease in pore interconnectivity as the temperature is increased. Fillion *et al.* reported that compact or nonporous ASW films can be grown at 120 K.[30] For $T \geqslant 140$ K, L_{Ps} increases again to ∼60 nm, consistent with the larger Ps diffusion coefficient in crystalline ice.[22] The temperature dependence of $F(0)$ mirrors that of L_{Ps}; as more Ps atoms escape into the vacuum $F(0)$ increases, and vice versa.

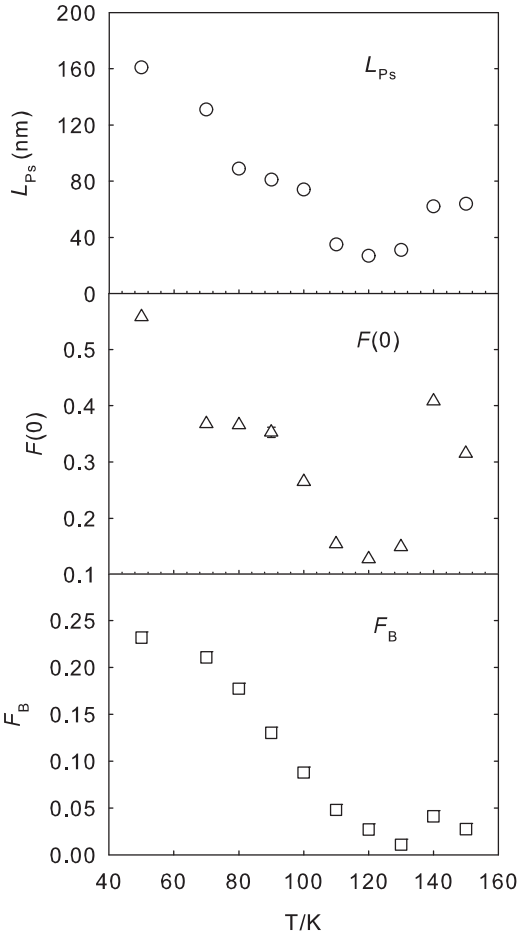

FIG. 6. Fitted effective o-Ps diffusion lengths L_{Ps}, $F(0)$ at the surface, and F_B in the bulk as a function of sample temperature.

F_B shows a temperature dependence similar to that of $F(0)$, reaching an asymptotic value close to zero, indicative of pore collapse. During crystallization above ∼135 K, $F(0)$ and F_B exhibit a sharp increase to values which change only slightly as the film is cooled to 50 K, confirming that the phase change is irreversible.

Preliminary results at $T = 170$ K indicate that $F(0)$ increases greatly and L_{Ps} is very low, which may be related to the much higher sublimation rate at this temperature. Further investigations are in progress and will be reported in the future.

The present VEPAS pore studies may be thought of as analogous to gas adsorption experiments.[3,10] The authors believe, however, that the parameter F is a more sensitive and direct measure of the porosity of ASW films.

The results of measurements of $S(T)$ for ASW films grown at different rates were shown in Ref. 24 and thus will not be reproduced here. However, it is worth reiterating here that the value of S for the bulk films reflects the mean size and concentration of closed pores, and that more closed pores are formed at higher growth rates. Further, a small increase in film S as T increases to 80 K followed by a decrease between 80 and 130 K indicates that S is sensitive to pore clustering and collapse, suggesting that its measurement may represent

a unique and sensitive probe of subnanometer closed pores in ice films.

D. Crystallization

Our previous paper[24] reported an unusual increase in S for the near-surface layer (thickness ∼80 nm) between 90 and 120 K, indicating a transition consistent with crystallization, which can be attributed to or driven by the reorganization of water molecules and/or the formation of ice islands at the surface, as reported in recent scanning tunneling microscopy (STM) observations of the surface layer.[31]

Both S and F for the bulk films increase when the films become crystalline between 130 and 140 K (Fig. 6 and Ref. 24). F is determined by pore interconnectivity and pore size (i.e., predominantly by growth temperature) and is relatively insensitive to other growth conditions, in contrast to S, which depends on the closed pore size and density in the ASW films. The increase in F may result from some o-Ps decay in larger closed pores, and possibly the diffusion of a small percentage of o-Ps atoms to the surface from the bulk as L_{Ps} in defect-free CI is long.[23] S in crystalline ice films is associated with two-γ decay processes, principally p-Ps, quenched o-Ps, and positrons in defect and bulk states. The change in S on crystallization depends on its initial value, which principally depends on the closed pore density and hence on the growth rate and temperature. The contribution of two-γ Ps annihilation before and after crystallization was studied by fitting Doppler-broadening spectra (i.e., Ge detector photopeaks centered at 511 keV) collected at 130 and 140 K and extracting the percentage contribution of the narrowest component (FWHM ≈ detector resolution). Such fitting yielded an increase in the component attributed to two-γ Ps decay from ∼3% to 7%, which is consistent with an increase in the measured S value.

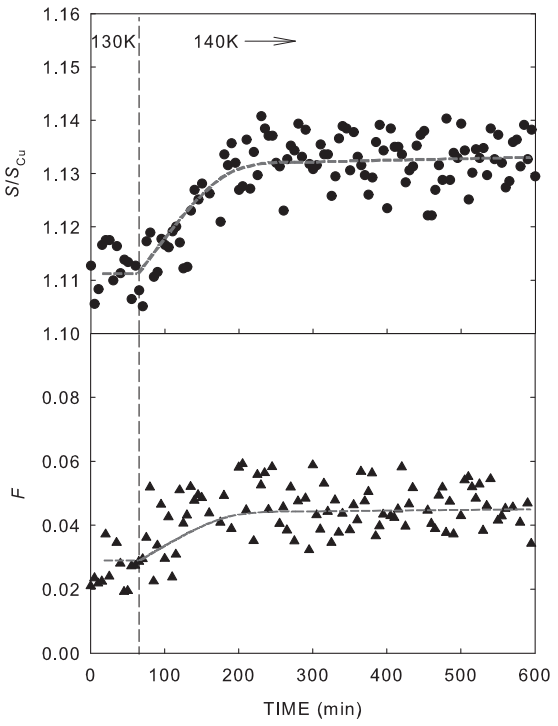

FIG. 7. Bulk film S (top) and F (bottom) as a function of time (500-s measurement time per point). $E = 10$ keV. After 65 min the temperature was raised from 130 to 140 K and crystallization begins. The lines are to guide the eye.

In order to observe the dynamics of the crystallization process at 140 K, F and S were measured as a function of time for an exemplar ASW film (Fig. 7). The data were taken via repeated 500-s runs at $E = 10$ keV, equivalent to a mean implanted depth of 1.7 μm. S is time independent at 130 K, but then at 140 K increases with time and towards an asymptotic value. F shows a much less pronounced behavior, consistent with our conclusion that S is much more sensitive to the phase of the ice than is F. We obtain from Fig. 7 a crystallization time (for complete conversion from ASW to CI) of ∼200 min, which is an order of magnitude shorter than that suggested by Kondo *et al.*[32] for thin (50 monolayer) ASW grown on single crystal Ru at 90 K, implying that there are interesting variations to be studied for films grown under different conditions, especially film thickness, substrate, and growth temperature—a conclusion supported by other earlier works (e.g., Refs. 33–35). It is clear that VEPAS could be developed into a sensitive and direct tool to observe the dynamics of ice film crystallization.

IV. CONCLUSIONS

The principal conclusions of this VEPAS study of structure-related properties of ASW and CI films are summarized here.

(i) *Growth of ASW and CI films*. The porosity of vapor-deposited ASW and CI films strongly depends on growth temperature, growth rate, and annealing temperature. 50-K-grown films are highly porous, reflected in the high values of the positron parameters S and F; 120-K-grown or annealed films are compact, but high S and low F values indicate the existence of many closed pores and a few open pores; 150-K-grown or annealed films are crystalline.

(ii) *Near-surface changes with time and temperature*. The Ps fraction F in the near-surface layers of freshly grown ASW and CI films decreases with time; for CI and annealed CI films, the near-surface F value is higher at higher measurement temperature. A possible mechanism for this behavior, based on changes in near-surface morphology, has been suggested.

(iii) *Annealing of open (interconnected) and closed pores*. The Ps fraction F is a sensitive and direct measure of the porosity of ASW films; for example, measurements of F suggest essentially complete annealing of mesopores at 120 K. The value of the S parameter for ice films is sensitive to the size and concentration of closed pores (from small clusters to ∼1 nm diam), and its measurement as a function of growth and annealing conditions therefore provides a unique method for investigating the formation and evolution of closed pores.

(iv) *Observation of crystallization processes*. Both S and F change irreversibly after crystallization, and first measurements of both parameters as a function of time as crystallization proceeds gives hope that VEPAS can be exploited to probe the energetics of crystallization.

The authors' ongoing research program on water ice films includes investigating the potential of VEPAS as a method for real-time observations of sublimation-related phenomena, further measurements to acquire semiquantitative information on pore size and concentration, and studies of the energetics of phase and structural changes.

ACKNOWLEDGMENTS

The authors are grateful to the China Scholarship Council for providing financial support for Y.C.W. during the performance of this research. This work was supported by the National Natural Science Foundation of China under Grant Nos. 10975110 and 51071111.

*P.G.Coleman@bath.ac.uk

[1] P. Jenniskens and D. F. Blake, Science **265**, 753 (1994).
[2] C. A. Angell, Science **319**, 582 (2008).
[3] K. P. Stevenson, G. A. Kimmel, Z. Dohnalek, R. S. Smith, and B. D. Kay, Science **283**, 1505 (1999).
[4] D. J. Safarik and C. B. Mullins, J. Phys. Chem. **121**, 6003 (2004).
[5] J. Cyriac and T. Pradeep, J. Phys. Chem. C **112**, 5129 (2008).
[6] R. S. Smith, C. Huang, E. K. L. Wong, and B. D. Kay, Surf. Sci. **367**, L13 (1996).
[7] E. H. G. Backus, M. L. Grecea, A. W. Kleyn, and M. Bonn, Phys. Rev. Lett. **92**, 236101 (2004).
[8] J.-H. Fillion, L. Amiaud, E. Congiu, F. Dulieu, A. Momei, and J.-L. Lemaire, Phys. Chem. Chem. Phys., **11**, 4396 (2009).
[9] M. S. Westley, G. A. Baratta, and R. A. Baragiola, J. Chem. Phys. **108**, 3321 (1998).
[10] U. Raut, M. Famá, B. D. Teolis, and R. A. Baragiola, J. Chem. Phys. **127**, 204713 (2007).
[11] U. Raut, B. D. Teolis, M. J. Loeffler, R. A. Vidal, M. Famá, and R. A. Baragiola, J. Chem. Phys. **126**, 244511 (2007).
[12] J. Shi, B. D. Teolis, and R. A. Baragiola, Phys. Rev. B **79**, 235422 (2009).
[13] T. Zubkov, R. S. Smith, T. R. Engstrom, and B. D. Kay, J. Chem. Phys. **127**, 184707 (2007).
[14] T. Zubkov, R. S. Smith, T. R. Engstrom, and B. D. Kay, J. Chem. Phys. **127**, 184708 (2007).
[15] L. Hornekar, A. Baurichter, V. V. Petrunin, D. Field, and A. C. Luntz, Science **302**, 1943 (2003).
[16] R. S. Smith, T. Zubkov, Z. Dohnalek, and B. D. Kay, J. Phys. Chem. B **113**, 4000 (2009).
[17] P. Ayotte, R. S. Smith, K. P. Stevenson, Z. Dohnalek, G. A. Kimmel, and B. D. Kay, J. Geophys. Res., [Planets] **106**, 33387 (2001).
[18] *Positron Beams and Their Applications*, edited by P. G. Coleman (World Scientific, Singapore, 2000).
[19] D. W. Gidley, W. E. Frieze, T. L. Dull, A. F. Yee, E. T. Ryan, and H. M. Ho, Phys. Rev. B **60**, R5157 (1999).
[20] R. Suzuki, T. Ohdaira, Y. Shioya, and T. Ishimaru, Jpn. J. Appl. Phys. **40**, L414 (2001).
[21] M. H. Weber and K. G. Lynn, in *Principles and Applications of Positron and Positronium Chemistry*, edited by Y. C. Jean, P. E. Mallon, and D. M. Schrader (World Scientific, Singapore, 2003), pp. 167–210.
[22] M. Eldrup, A. Vehanen, P. J. Schultz, and K. G. Lynn, Phys. Rev. Lett. **51**, 2007 (1983).
[23] M. Eldrup, A. Vehanen, P. J. Schultz, and K. G. Lynn, Phys. Rev. B **32**, 7048 (1985).
[24] Y. C. Wu, A. Kallis, J. Jiang, and P. G. Coleman, Phys. Rev. Lett. **105**, 066103 (2010).
[25] C. L. Wang, M. H. Weber, and K. G. Lynn, J. Appl. Phys. **99**, 113514 (2006).
[26] N. B. Chilton and P. G. Coleman, Meas. Sci. Technol. **6**, 53 (1995).
[27] A. van Veen, H. Schut, J. de Vries, R. A. Hakvoort, and M. R. Ijpma, AIP Conf. Proc. **218**, 171 (1990).
[28] M. Eldrup, A. Vehanen, P. J. Schultz, and K. G. Lynn, Phys. Rev. Lett. **53**, 954 (1984).
[29] N. J. Sack and R. A. Baragiola, Phys. Rev. B **48**, 9973 (1993).
[30] J.-H. Fillion, L. Amiaud, E. Congiu, F. Dulieu, A. Momeni, and J.-L. Lemaire, Phys. Chem. Chem. Phys. **11**, 4396 (2009).
[31] M. Mehlhorn and K. Morgenstern, New J. Phys. **11**, 093015 (2009).
[32] T. Kondo, H. S. Kato, M. Bonn, and M. Kawai, J. Phys. Chem. C **126**, 181103 (2007).
[33] Z. Dohnalek, G. A. Kimmel, R. L. Ciolli, K. P. Stevenson, R. S. Smith, and B. D. Kay, J. Chem. Phys. **112**, 5932 (2000).
[34] D. J. Safarik, R. J. Meyer, and C. B. Mullins, J. Chem. Phys. **118**, 4660 (2003).
[35] D. J. Safarik and C. B. Mullins, J. Chem. Phys. **121**, 6003 (2004).